Structure
Article

# Symmetrical Modularity of the COP9 Signalosome Complex Suggests its Multifunctionality

Michal Sharon,[1,3] Haibin Mao,[2] Elisabetta Boeri Erba,[1] Elaine Stephens,[1] Ning Zheng,[2] and Carol V. Robinson[1,*]
[1]Department of Chemistry, University of Cambridge, Lensfield Road, Cambridge CB2 1EW, UK
[2]Department of Pharmacology, University of Washington, Seattle, WA 98195-7280, USA
[3]Present address: Department of Biological Chemistry, Weizmann Institute of Science, Rehovot 76100, Israel.
*Correspondence: cvr24@cam.ac.uk
DOI 10.1016/j.str.2008.10.012

## SUMMARY

**The COP9 signalosome (CSN) is an eight-subunit protein complex that is found in all eukaryotes. Accumulating evidence indicates its diverse biological functions that are often linked to ubiquitin-mediated proteolysis. Here we applied an emerging mass spectrometry approach to gain insight into the structure of the CSN complex. Our results indicate that the catalytically active human complex, reconstituted in vitro, is composed of a single copy of each of the eight subunits. By forming a total of 35 subcomplexes, we are able to build a comprehensive interaction map that shows two symmetrical modules, Csn1/2/3/8 and Csn4/5/6/7, connected by interactions between Csn1-Csn6. Overall the stable modules and multiple subcomplexes observed here are in agreement with the "mini-CSN" complexes reported previously. This suggests that the propensity of the CSN complex to change and adapt its subunit composition might underlie its ability to perform multiple functions in vivo.**

## INTRODUCTION

The COP9 signalosome (CSN) is an evolutionary conserved multifunctional complex (Chamovitz et al., 1996; Wei et al., 1994, 1998). It contains eight core subunits, named Csn1–8, in order of decreasing molecular weight (Deng et al., 2000). The complex has been shown to regulate diverse cellular processes, ranging from cell-cycle progression and signal transduction to transcriptional regulation (for reviews see Cope and Deshaies, 2003; Harari-Steinberg and Chamovitz, 2004; Schwechheimer, 2004; von Arnim, 2003; Wolf et al., 2003). Despite the wide spectrum of CSN functions, a common theme has become apparent suggesting that many of these functions are tied to the ubiquitin-mediated proteolysis pathway. Several studies have shown that the CSN regulates the activity of cullin-RING E3 ligases (CRL) by removal of the ubiquitin-like protein Nedd8 from the cullin subunit of the cullin containing E3 ligases. Cycles of neddylation and deneddylation of cullins appear to be needed to sustain their ubiquitinating activity.

The intact eight-subunit CSN complex is composed of six PCI (for *p*roteasome, *C*OP9, and *i*nitiation factor 3) domains found in Csn1, Csn2, Csn3, Csn4, Csn7, and Csn8. Csn5 and Csn6 contain an MPN domain (for *M*pr1p and *P*ad1p *N*-terminal) (Aravind and Ponting, 1998; Glickman et al., 1998; Hofmann and Bucher, 1998). The deneddylation activity is linked to the metalloprotease motif ($EX_nHXHX_{10}D$) of Csn5, which is embedded within the MPN domain and known as JAMM (*JA*B1/*M*PN/*M*ov34) or MPN+ motif (Cope et al., 2002; Maytal-Kivity et al., 2002b). The structure of the JAMM domain has been solved and additional amino acids outside of the domain have been shown to be essential for the deneddylation reaction (Ambroggio et al., 2004). Orthologous CSN complexes have been identified in higher eukaryotes with all eight subunits being encoded (reviewed in Wei and Deng, 2003).

The PCI and MPN domains are found almost exclusively in two other large protein complexes: the 19S lid of the 26S proteasome and the eukaryotic translation initiation factor eIF3. The 26S proteasome is composed of the 20S catalytic core particle and the 19S regulatory particle (Voges et al., 1999). The lid is a subcomplex of the 19S located at the exterior ends of the 26S proteasome, and it is required for protein selection and deubiquitination by Rpn11, an MPN subunit. eIF3 promotes the formation of pre-initiation complexes by interacting with other initiation factors, and facilitates loading of the 40S subunit onto the ternary eIF2-tRNA-Met-GTP complex (Hinnebusch, 2006). The CSN exhibits a remarkable one-to-one similarity to subunits of the proteasome lid (Glickman et al., 1998), suggesting that CSN and the lid might have a common evolutionary ancestor. The eIF3 complex, however, is more distantly related and contains 6 PCI and 2 MPN proteins among its 13 components (Damoc et al., 2007; Hinnebusch, 2006). Recent studies indicate physical interactions among the lid, eIF3, and CSN complexes (Huang et al., 2005; Peng et al., 2003; Schwechheimer and Deng, 2001), leading to proposals that the CSN acts as an alternative lid for the 26S proteasome (Deshaies and Meyerowitz, 2000; Li and Deng, 2003) and might regulate eIF3 levels (Yahalom et al., 2008).

A large number of proteins have been reported to associate with the CSN complex (Richardson and Zundel, 2005; Wei and Deng, 2003). Currently it is unclear whether all these proteins are degradation targets or if they have other roles. Moreover, numerous investigations have shown that disruption or knockdown of one of the CSN subunit does not necessarily result in the same phenotype as nullification or genetic modification of other individual subunits (Bemis et al., 2004; Mundt et al., 2002; Oron et al., 2002; Peth et al., 2007; Tomoda et al., 2002). This implies that some CSN subunits have other physiological roles in addition to being a component of the CSN complex.

**Table 1. Theoretical and Measured Masses of Protein Subunits**

| Csn Subunit | Theoretical Mass (Da) | Experimental Mass (Da) mass (Da) |
|---|---|---|
| Csn1 | 52,510 | 52,492 ± 4 |
| Csn2 | 48,920 | 48,920 ± 4 |
| Csn3[a] | 46,615 | 46,611 ± 5 |
| Csn3 | 45,709 | 45,708 ± 2 |
| Csn4 | 46,493 | 46,493 ± 2 |
| Csn5[b] | 38,688 | 38,717 ± 5 |
| Csn5[c] | 38,753 | 38,776 ± 2 |
| Csn6 | 33,800 | 33,799 ± 2 |
| Csn6[d] | 33,392 | 33,392 ± 9 |
| Csn7a[e] | 30,794 | 30,796 ± 3 |
| Csn7b | 27,034 | 27,042 ± 1 |
| Csn8 | 23,450 | 23,449 ± 1 |

All masses, except those indicated otherwise, were measured using the accurate mass method.
[a] Csn3 version a (see Supplemental Experimental Procedures) measured using a $C_{18}$ pipette (Zip Tip).
[b] Measured under denaturing conditions using a $C_{18}$ pipette (ZipTip).
[c] Csn5 has a bound Zn atom, measured under native conditions.
[d] Csn6 different strain ΔLFF C-terminal (Zip Tip).
[e] Measured from tandem MS spectra.

Biochemical size fractionation analysis indicates that few CSN subunits are monomeric or in smaller versions of the CSN ("mini-CSNs"). Interestingly, Csn5 the active CSN subunit, is a common component of many of the small CSN complexes (reviewed in Chamovitz and Segal, 2001), and a large fraction of overexpressed Csn5 is found in the free form (Tomoda et al., 2002). Although the CSN-associated Csn5 is mostly nuclear, the free form of Csn5 appears to be both cytoplasmic and nuclear (Tomoda et al., 2002), and the latter might reflect a nuclear export activity for Csn5. Whether individual CSN subunits, or the mini-CSNs, have independent activities, explaining the diverse functionality of the CSN complex, is unclear.

Despite the increasing list of biochemical functions assigned to the CSN, to date there is no information regarding the structural arrangement of individual subunits. A high-resolution structure of CSN has not been reported; however, a low-resolution electron microscopy analysis of the purified human CSN is available, indicating a dynamic particle (Kapelari et al., 2000). In addition, known pair-wise interactions of CSN subunits (summarized in Wei and Deng, 2003) provide clues about aspects of subunit organization. Recently we have solved the structural organization of the nine-component 19S lid by coupling tandem mass spectrometry (MS) with cross-linking experiments (Sharon et al., 2006). A natural continuation will be to study the subunit topology of the related CSN complex and compare this with our interaction map of eIF3 determined recently (Zhou et al., 2008). A map of subunit interactions and information about the overall stability of various subcomplexes enables insight into the stable modules of these complexes, which highlight potential functional subcomplexes as well as the contribution of individual subunits to the overall activity. Models of the subunit architecture form the basis for further biochemical studies and are especially significant when high-resolution structures of these dynamic complexes remain elusive. To deduce our model of the CSN, we reconstituted the human complex by coexpression in *Escherichia coli* of Csn1/2/3 and Csn4/6/7 and single expression of Csn5 and Csn8. This strategy enabled us to form the intact eight-subunit complex. We confirmed the activity of this intact complex, together with various subcomplexes, using a deneddylation assay of neddylated cullin1 (see Supplemental Data available online) and applied a mass spectrometry (MS) approach that maintains protein complexes in their native state (Benesch et al., 2007; Sharon and Robinson, 2007; van den Heuvel and Heck, 2004).

Our results show that the complex contains a single copy of all eight subunits. We also noted that the interactions of the seven-subunit complex are maintained in solution, even without the active Csn5 subunit. Furthermore, we discovered the tendency of the CSN to readily dissociate to form smaller subcomplexes. By combining the MS and tandem MS results and using a network inference algorithm, we generated a complete subunit interaction map containing all eight subunits of the CSN complex. Two symmetrical protein modules become apparent from the model, highlighting the possible origin of a number of the mini-CSN complexes reported previously. More remarkable is that similarities in subunit interactions are revealed when we compare our models of the yeast 19S lid, the human COP9 signalosome, and human eIF3 complexes.

## RESULTS

### Correlating the Identity of the Protein Subunit with Its Intact Mass

The ability to relate the accurate mass of a protein subunit to the sequence of the protein is the fundamental premise upon which our model-building takes place. The standard proteomics method that is often used catalogs all proteins within the sample and enables their identification in databases (Mann et al., 2001). However, without the correlation between accurate mass and sequence, it is often ambiguous as to which protein subunit is present within a particular subcomplex. Moreover, protein subunits are invariably truncated and modified to such an extent that identification based on intact mass alone is ambiguous. Therefore, we have developed an approach in which each subunit is identified by its unique mass and sequence simultaneously (see Experimental Procedures and Figure S2). Using this approach, subunits and subcomplexes can be assigned unambiguously. The mass of the Csn5 subunit was determined independently (Table 1). The remaining seven CSN subunits were separated chromatographically and the masses of the individual proteins, together with peptide identification, enabled us to identify and assign each subunit by its unique mass (Table 1).

### Composition of the Intact CSN and Its Subcomplexes

As a basic prerequisite for studying the structural properties of the CSN complex, we first investigated the activity of the reconstructed human complex using a deneddylation assay. We incubated at 20°C neddylated cullin1 at 1:50 of CSN:Nedd-cullin1 with (i) Csn5, (ii) Csn4/6/7 plus Csn5, (iii) Csn1/2/3 together with Csn5 and Csn8, (iv) the wild-type eight-subunit complex, and (v) the intact complex with various constructs of subunit Csn7. Results showed that for the intact CSN ~50% of the

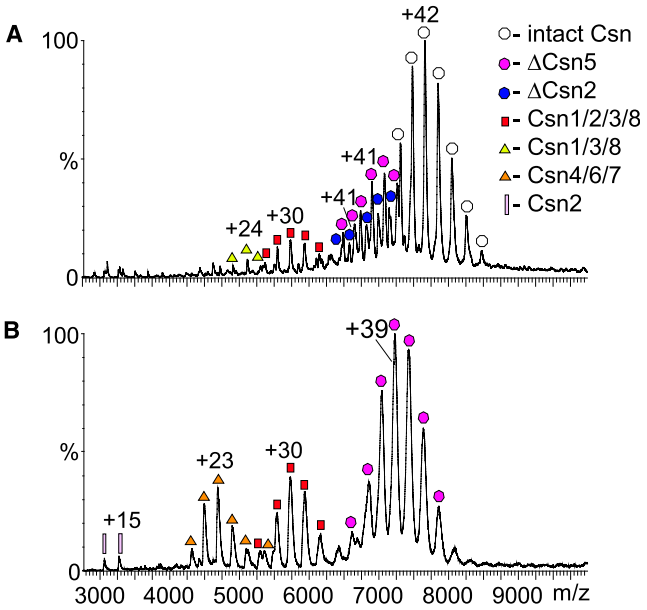


**Figure 1. Electrospray Mass Spectra of the Intact CSN Complexes**

(A) Mass spectrum of the intact eight-component CSN complex. The predominant species, in the range of 7250–8250 m/z, is assigned to the intact eight-subunit complex. Additional well-resolved charge states are observed between 6250 and 7250 m/z, corresponding in mass to substoichiometric complexes from which either Csn2 or Csn5 have dissociated. Two additional subcomplexes, assigned to Csn1/3/8 and Csn1/2/3/8, give rise to signals centered at 5000 and 5750 m/z, respectively.

(B) MS spectrum recorded for the ΔCsn5 complex in which Csn5 is absent. The major charge series in the range of 6500 to 8000 m/z corresponds in mass to the seven-subunit complex. In addition, in the absence of Csn5, two stable subcomplexes are detected, Csn4/6/7 and Csn1/2/3/8, centered at 4500 and 5750 m/z, respectively.

**Table 2. Theoretical and Measured Masses of Complexes and Subcomplexes Identified in MS Analysis**

| Subcomplex | Theoretical Mass (Da) | Experimental Mass (Da) mass (Da) |
|---|---|---|
| Intact mass[a] | 320,841 | 321,274 ± 35 |
| Δ2[a] | 271,921 | 272,587 ± 25 |
| Δ3[a] | 274,229 | 276,140 ± 21 |
| Δ5[b] | 277,903 | 278,153 ± 13 |
| Δ8[a] | 297,391 | 298,081 ± 74 C13188H20924N3580O3987S126 |
| Δ5Δ2[b] | 228,983 | 229,120 ± 8 |
| Δ5Δ3[b] | 232,195 | 232,317 ± 31 |
| Δ5Δ8[b] | 254,454 | 254,601 ± 20 |
| Δ2Δ5Δ8[b] | 205,534 | 205,982 ± 31 |
| Csn4/5/6/7[b] | 146,022 | 146,285 ± 5 |
| Csn1/2/3/8[b] | 170,569 | 170,649 ± 10 |
| Csn1/4/6/8[b] | 156,233 | 156,264 ± 4 |
| Csn1/2/3[b] | 147,120 | 147,144 ± 15 |
| Csn1/3/8[b] | 121,649 | 121,697 ± 6 |
| Csn4/6/7[b] | 107,334 | 107,343 ± 10 |
| Csn1/2[b] | 101,412 | 101,404 ± 41[c] |
| Csn3/8[b] | 69,157 | 69,186 ± 8 |
| Csn4/7[b] | 73,535 | 73,567 ± 10 |
| Csn6/7[b] | 60,841 | 60,852 ± 7 |

Two different preparations of the complex containing different subunit isoforms were used in the analysis (footnotes a and b) (see also Supplemental Data for sequences). The superscript above each complex or subcomplex designates the isoforms (see Table 1).

[a] Csn3[a] (46,612 Da), Csn6[d] (33,392 Da), Csn7a[e] (30,794 Da).

[b] Csn7b (27,034 Da), Csn3 (45,709 Da), Csn6 (33,800 Da).

[c] In the majority of cases the experimental mass is greater than the theoretical mass because water and buffer ions are often trapped within the macromolecular ions. In some instances the mass is slightly lower, but in all cases this is within the error of the experimental measurement.

cullin1 was deneddylated within 10 min (Figure S1). For the intact complex containing different isoforms of Csn7 the activity of the Csn7b-containing complex was indistinguishable from that consisting Csn7a. The only difference was that Csn7a was marginally slower than wild-type with ~50% deneddylation achieved after 30 min. The small subcomplexes (i) to (iii) showed no appreciable activity in this assay. These results allow us to conclude that the reconstituted CSN complex has appreciable catalytic activity.

An electrospray mass spectrum recorded for an aqueous solution of the eight-subunit CSN complex showed a major series of peaks assigned to the charge states of the intact complex with a mass of (321,274 ± 35 Da) confirming that all eight subunits are present at unit stoichiometry (Figure 1A and Table 2). Interestingly, for this complex we also observe a series of lower-molecular-weight species under MS conditions where most protein complexes remain intact (Sharon and Robinson, 2007). These are assigned predominantly to substoichiometric complexes in which Csn2 and Csn5 are absent. This indicates that both subunits have weaker interactions with other subunits, and that they are peripheral and hence dissociate at the lowest activation energies. Interestingly, we could also detect in the MS spectra smaller subcomplexes corresponding to Csn1/2/3/8 and Csn1/3/8. This implies that this complex is considerably less stable than the majority of complexes that we have studied to date. Consistent with this idea is that if we examine the complex in the absence of Csn5, a seven-subunit complex is detected. However, we find that in this case, under the same MS conditions, more extensive dissociation has occurred yielding smaller subcomplexes (Figure 1B). The solution phase products include Csn1/2/3/8, observed in Figure 1A, and a stable trimer Csn4/6/7. These results imply that binding of Csn5 confers stability to the complex in solution.

To probe proteins at the core of the complex and to define all possible protein-protein interactions, we generated sets of overlapping subcomplexes (Hernandez et al., 2006). This was done by stepwise addition of methanol to the complex-containing solutions, reasoning that this would disrupt hydrophobic interactions and generate additional subcomplexes. A wide range of subcomplexes was produced including heptamers, hexamers, tetramers, trimers, dimers, and monomers (Figures 2A and 2B). Under these conditions the Csn1/2/3/8 tetramer persists, together with a smaller trimer Csn1/3/8, implying a particular stability for this network of interactions. By contrast, the Csn(5)/4/6/7 subcomplexes are of lower intensity and individual subunits are more prevalent in the spectra, implying a reduced stability within Csn4/5/6/7 compared with that observed for Csn1/2/3/8.

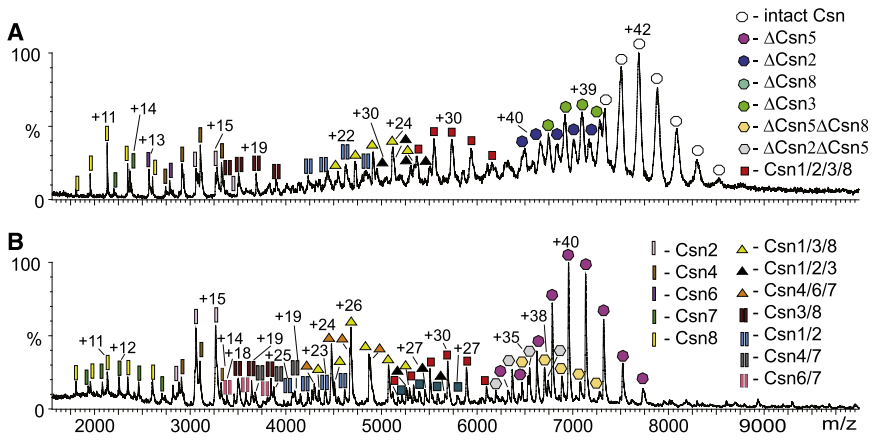


**Figure 2. High-Energy MS Spectrum of the CSN Complex**

Harsh conditions were employed to induce disruption of the complexes both in solution (by addition of up to 10% methanol) and in the gas phase (by increasing the accelerating voltage). Spectra recorded for the eight-component complex (A) and for the ΔCsn5 complex (B) are shown.

We assigned the subcomplexes based on their intact masses and confirmed the assignment using tandem MS (MS/MS). In this method, a specific well-defined mass-to-charge ratio (m/z) that encompasses the parent ion is selected and accelerated through a collision cell at increased pressures of argon collision gas. The process gives rise to multiple collisions in which the internal energy of the ions accumulates. Dissociation occurs when this energy reaches a threshold value, yielding product ions. This dissociation process involves unfolding of a peripheral subunit that is released from the complex as a highly charged individual protein subunit (Benesch et al., 2006). Concomitantly "stripped" complexes are formed with lower charge than the original complex. Practically, therefore, this enables at least one protein component of the complex to be identified through the subunit released. Moreover, the narrowing of the peaks due to the loss of adduct ions increases the accuracy of the mass measurement over those of inactivated complexes (McKay et al., 2006). As a final check on the consistency of the assignment, both masses and charges of the monomeric subunits expelled from the assembly and the stripped complexes formed sum to the mass and charge of the original ion isolated for tandem MS.

By applying the tandem MS strategy to the intact and ΔCsn5 complexes and isolating a wide range of values covering the features of the mass spectrum, we identified 26 different subcomplexes (Table 3). For example, to examine the composition of the 170.6 kDa subcomplex, an MS/MS spectrum was acquired for the 29+ charge state (Figure 3A). Two series of ions are observed at the low-m/z region (left-hand side of the spectrum), assigned according to their measured mass to Csn3 and Csn8. The corresponding stripped complexes are centered at 8,000 and 12,000 m/z and their masses are consistent with Csn1/2/3 and Csn1/2/8. By using extrapolation, we can therefore conclude that before collisional activation the subcomplex is a tetramer composed of Csn1/2/3/8. A more complicated spectrum is shown in Figure 3B. The data were obtained by isolating ions at 7000 m/z, giving rise to the dissociation of the individual subunits Csn3, Csn4, Csn7, and Csn8 at the low-m/z region (Csn8 is not labeled in the figure). In the high-m/z region of the spectrum, charge states of both hexamers and pentamers are identified, all containing Csn1 and Csn6. The assignment process reveals that the peaks isolated arise from a number of overlapping ions ΔCsn5, ΔCsn2ΔCsn5, and ΔCsn5ΔCsn8. Overall, from our MS/MS experiments we can conclude that Csn7, Csn4, Csn3, and Csn8 dissociate readily from the intact complex. Similarly, Csn3 and Csn8 also dissociate readily from the Csn1/2/3/8, indicating their peripheral position in both the intact and tetrameric complexes. Csn2 and Csn4 are also observed, but not as readily. Interestingly, careful analysis of all the MS/MS data generated using the intact CSN and ΔCsn5 complexes (Table 3) revealed that Csn1 and Csn6 are not dissociated from either complex, suggesting that these subunits are located within the core.

To probe the stability and integrity of the various subcomplexes identified in our experiments, we attempted to reassemble in vitro a number of these subcomplexes from the complexes produced by our coexpression and single-expression protocols. Initially we analyzed two inactive trimers, Csn1/2/3 and Csn4/6/7, and compared their stability in the mass spectra. Interestingly, the subcomplex Csn4/6/7 was found to be very stable and able to self-associate to form dimers and trimers of Csn4/6/7, which is in line with our previous observation. By contrast, spectra recorded for the Csn1/2/3 trimer showed populations of Csn1/2, Csn1/3, and Csn1/2/3, emphasizing its tendency to dissociate in the absence of other subunits (data not shown). Incubating the two trimers, Csn1/2/3 and Csn4/6/7, led to the formation of a well-defined hexamer with a measured mass corresponding to Csn1/2/3/4/6/7 (Figure 4A). By contrast, incubation of Csn1/2/3/4/6/7/8 with Csn5 and MS of the resulting solution showed that it was not possible to reconstitute the intact eight-component complex in this way. However, it was possible to form a Csn4/5/6/7 tetramer (Figure 4B), which was confirmed by the observation of Csn4/5/6 and Csn5/6/7 subcomplexes, the latter after gas phase dissociation of Csn7 and Csn4, respectively. In summary, these results show that Csn5 could not be integrated into the seven-subunit complex but could assemble with the Csn4/6/7 trimer to form the tetramer Csn4/5/6/7. Interestingly, however, the predominant species in this spectrum is the Csn4/6/7 trimer, suggesting that interactions of Csn5 are enhanced by the presence of the second module. This observation is in line with our previous finding that dissociation of the Csn4/6/7 trimer is not observed in solutions of the eight-subunit complex but the trimer is readily dissociated in the absence of Csn5, implying a role for Csn5 in stabilizing the interactions between the two modules.

## Calculating an Interaction Network

To define a comprehensive interaction network of the CSN complex, a total of 35 subcomplexes (Tables 1 and 2), which were identified from the MS and MS/MS data, were submitted

**Table 3. Theoretical and Measured Masses of Complexes and Subcomplexes Identified in Tandem MS Analysis**

| Subcomplex | Theoretical Mass (Da) | Experimental Mass (Da) mass (Da) |
|---|---|---|
| Δ3[a] | 274,229 | 274,395 ± 58 |
| Δ7[a] | 290,047 | 290,147 ± 24 |
| Δ8[a] | 297,391 | 297,284 ± 27[d] |
| Δ2Δ3[a] | 225,309 | 225,589 ± 5 |
| Δ3Δ7[a] | 243,435 | 243,616 ± 32 |
| Δ3Δ8[a] | 250,779 | 250,652 ± 67[d] |
| Δ5Δ2[b] | 228,983 | 228,970 ± 48[d] |
| Δ5Δ3[b] | 232,195 | 232,200 ± 6 |
| Δ5Δ4[b] | 231,410 | 231,431 ± 20 |
| Δ5Δ7[b] | 250,861 | 250,905 ± 12 |
| Δ2Δ3Δ5[b] | 183,275 | 183,262 ± 35[d] |
| Δ3Δ5Δ8[b] | 208,746 | 208,739 ± 7 |
| Δ3Δ7Δ8[a] | 219,985 | 220,217 ± 40 |
| Δ5Δ7Δ8[b] | 227,412 | 227,433 ± 22 |
| Δ4Δ5Δ8[b] | 207,961 | 207,957 ± 45[d] |
| Csn1/6/7/8[b] | 136,782 | 136,783 ± 15 |
| Csn1/2/3[b] | 147,120 | 147,149 ± 16 |
| Csn1/2/8[b] | 124,861 | 124,869 ± 7 |
| Csn4/5/6[b] | 118,980 | 119,125 ± 25 |
| Csn5/6/7[b] | 99,529 | 99,918 ± 31 |
| Csn1/2 | 101,412 | 101,423 ± 1 |
| Csn1/3[b] | 98,200 | 98,191 ± 8 |
| Csn3/8[b,c] | 69,157 | 69,158 ± 8 |
| Csn4/6[b] | 80,292 | 80,372 ± 3 |
| Csn4/7[b] | 73,535 | 73,583 ± 7 |
| Csn6/7[b] | 60,841 | 60,887 ± 25 |

Two different preparations containing different subunit isoforms were used in the analysis (footnotes a and b) (see Supplemental Data for sequences). The superscript above each complex or subcomplex designates the isoforms (see Table 1):

[a] Contains wild-type subunits, with the exception of Csn3[a] (46,612 Da), Csn6[d] (33,392 Da), and Csn7a[e] (30,794 Da).

[b] Contains wild-type subunits, with the exception of Csn7b, Csn3 (45,709 Da), and Csn6 (33,800 Da).

[c] Dissociate together in MS/MS.

[d] In the majority of cases, the experimental mass is greater than the theoretical mass because water and buffer ions are often trapped within the macromolecular ions. In some instances the mass is slightly lower, but in all cases this is within the error of the experimental measurement.

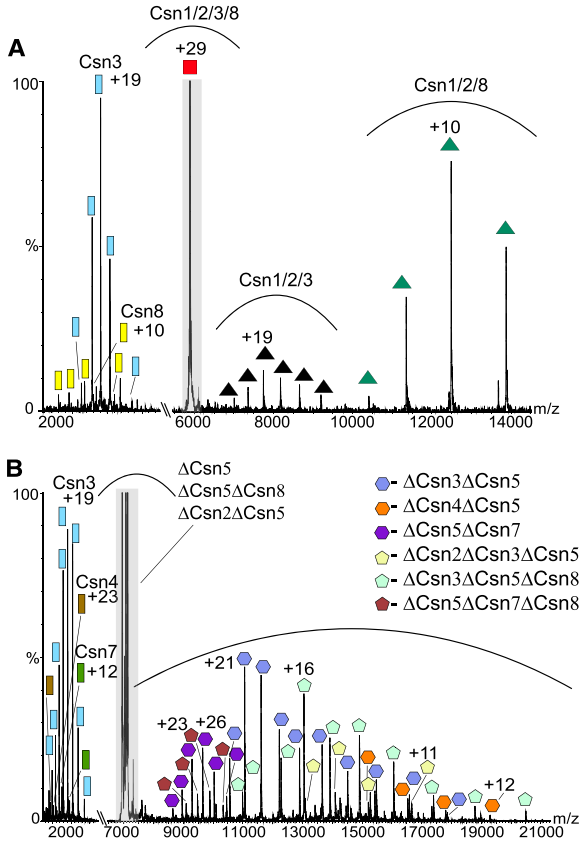


**Figure 3. Tandem MS Analysis of the Subcomplexes**

(A) Isolation at 5900 m/z of the 29+ charge state. Peaks centered at 8000 m/z correspond to the loss of the Csn8 subunit (black), whereas the series at 10,500–14,400 m/z correspond to the loss of the Csn3 subunit (green). At low m/z 1600–3000 series of peaks are assigned to the corresponding individual subunits, Csn8 (yellow), and Csn3 (light blue) subunits. By extrapolation we could conclude that the subcomplex is composed of four subunits (Csn1/Csn2/Csn3/Csn8).

(B) MS/MS spectrum showing the dissociation products of ions isolated at 7000 m/z. Charge states above 7000 m/z correspond to "stripped" complexes in which one individual subunit has been dissociated from the complex. The individual stripped subunits are observed at the low m/z values. Based on the analysis of the spectrum, we could conclude that a mixed population of ions (ΔCsn5, ΔCsn2ΔCsn5, and ΔCsn5ΔCsn8) was originally isolated. The different species are labeled.

to SUMMIT (Taverner et al., 2008). This algorithm determines the shortest path network that connects all subunits with their interaction partners. Within the set of overlapping subcomplexes, 6 were dimers, 6 trimers, 4 tetramers, 6 pentamers, and 13 were hexameric or larger. A subset of these subcomplexes generated for the ΔCsn5 complex, together with their topological arrangement, is shown in Figure 5A. Interestingly, all seven subunits are readily observed in various overlapping subcomplexes, even over this narrow mass spectral range (3000 m/z units); consequently, this increases our probability of finding a unique solution to the interaction network. It is also noteworthy that the list of 35 subcomplexes is well above the minimum number required to define interactions within protein complexes (Taverner et al., 2008). As such, all interactions within the eight-subunit CSN complex were predicted with a weighted average of 100% leading to a high confidence interaction map (Figure 5B).

This interaction network clearly shows two distinct modules. The first includes Csn1, Csn2, Csn3, and Csn8, whereas the second module contains Csn4, Csn5, Csn6, and Csn7. The interactions that link the two modules are between Csn1 and Csn6. The structural organization of the two modules is highly symmetrical; three subunits form protein-protein interactions with each other (Csn1/3/8 and Csn4/6/7) and two additional subunits (Csn2 and Csn5) form stable protein-protein interactions with only one other subunit (Figure 5B). This structural arrangement explains our observation that Csn4/6/7 forms a more stable

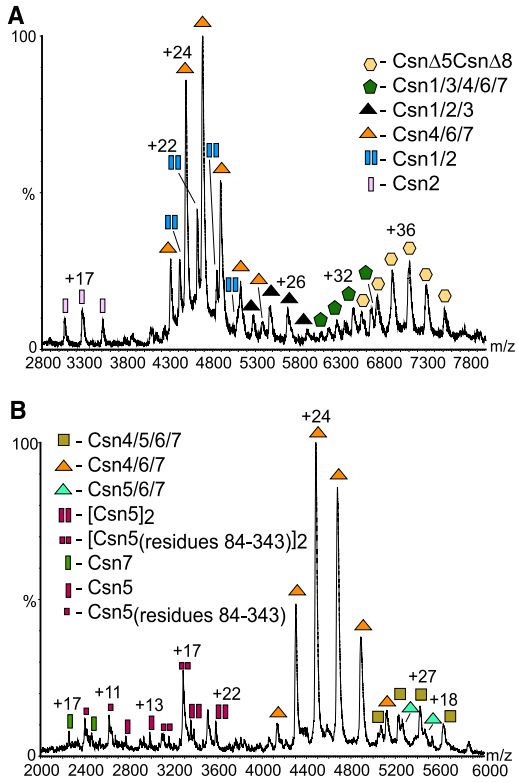


**Figure 4. Monitoring Subcomplex Association**

(A) Mass spectrum revealing the interaction between the two subcomplexes (Csn1/2/3 and Csn4/6/7). Charge series corresponding to the hexameric particle, Csn1/2/3/4/6/7 (ΔCsn5ΔCsn8), are observed between 6800 and 7600 m/z. The dissociation of this hexamer into the individual Csn2 subunit and its corresponding pentamer Csn1/3/4/6/7 is also detected.

(B) Mass spectrum acquired 105 min after incubating Csn5 with Csn4/6/7. The formation of a Csn4/5/6/7 subcomplex could be probed (charge series centered at 5400 m/z) along with an additional smaller subcomplex that corresponded in mass to Csn5/6/7.

complex than Csn1/2/3. Each subunit within the Csn4/6/7 subcomplex forms interactions with two subunits, whereas in the Csn1/2/3 subcomplex only Csn1 forms interactions with two subunits. Moreover, the observation that neither Csn1 nor Csn6 is dissociated from the complex during tandem MS analysis is explained because both form a hub, each with three interacting subunits.

## DISCUSSION

We have shown from a series of MS experiments that all subunits in the reconstituted human CSN are present at unit stoichiometry leading to a measured mass of 321 kDa. It was previously reported that the CSN fractionates as a 450–550 kDa complex during gel filtration (Wei and Deng, 2003). The discrepancy is indicative of an irregular nonglobular shape, consistent with our findings of two distinct modules with few connecting links between them. From our experiments we were also able to determine that Csn5 is not necessary for the integrity of the complex, which is in accord with previous observations (Dohmann et al., 2005; Oron et al., 2002; Tomoda et al., 2002). However, Csn5 was found to confer additional stability to the complex. Moreover, we could identify additional substoichiometric complexes present in solution as ΔCsn2, ΔCsn8, ΔCsn2ΔCsn5, and ΔCsn5ΔCsn8, implying labile interactions between these subunits and the core of the complex. By coupling the MS and tandem MS results and submitting them to a network inference algorithm, we calculated an interaction network for the eight-component human CSN complex (Figure 5). Interestingly, the complex is composed of two modules, Csn1/2/3/8 and Csn4/5/6/7, connected by interactions between Csn1 and Csn6. Within each module, three of the subunits (Csn1/3/8 and Csn4/6/7) form compact trimers, both binding to additional subunits Csn2 and Csn5, respectively.

It is of interest to compare our interaction network with those published previously for the CSN from various sources. Numerous pairwise interactions were reported for the CSN from fungi, *Arabidopsis*, *Drosophila*, fission yeast, and humans using the yeast two-hybrid system and filter binding assays (reviewed in Wei and Deng, 2003). In total, 25 pairwise interactions were detected forming a dense web of protein-protein interactions. Out of the nine pairwise interactions observed in our model, eight were detected in the yeast two-hybrid method. Three additional interactions, Csn2/5, Csn3/4, and Csn7/8, identified in the yeast two-hybrid study, could occur if the two modules came into contact through rotation about the Csn1:Csn6 plane of interaction. We attribute the additional 14 reported interactions to the fact that transient interactions would not be detected by our methods as well as the tendency of the two-hybrid system to produce false positives (Uetz et al., 2000). For example, Csn8, the smallest subunit (23.5 kDa), was reported to form five protein-protein interactions. A second potential problem is that endogenous proteins might facilitate two-hybrid interactions that are not direct, and the presence of endogenous proteins might confuse the analysis. For instance, Csn5 binds to Gal4 and this might turn up as false positive in two hybrid assays (Nordgard et al., 2001). Moreover, it is noteworthy that yeast comprises endogenous PCI and MPN, proteins that might act as a bridge and interfere with the assay; specifically, a C-terminal fragment of human Csn1 has been shown to interact with yeast signaling molecules (Spain et al., 1996). A fundamental advance of our MS approach is that subunits that are in direct, stable interactions are identified, and heterogeneity and subcomplex formation are apparent from the spectra.

Our results highlight several aspects concerning the biogenesis pathway of the COP9 signalosome. The crucial role of Csn1 in complex integrity was demonstrated previously: complete loss of Csn1 in *Arabidopsis* abolishes accumulation of Csn8, dissociates Csn5 from the complex, and leads to a significant reduction in the levels of Csn4 and Csn7 (Tsuge et al., 2001; Wang et al., 2002b). Likewise, complete depletion of Csn6 resulted in the loss of the CSN complex and redistribution of some CSN subunits into subcomplexes accompanied by instability of Csn1, Csn3, Csn4, Csn7, and Csn8 (Gusmaroli et al., 2007; Peth et al., 2007). A recent study demonstrated that knockdowns of Csn1 and Csn3 cause a proportional reduction in all CSN subunits and a decrease in the levels of the holocomplex (Peth et al., 2007). Our results, together with the deletion experiments described above, highlight the

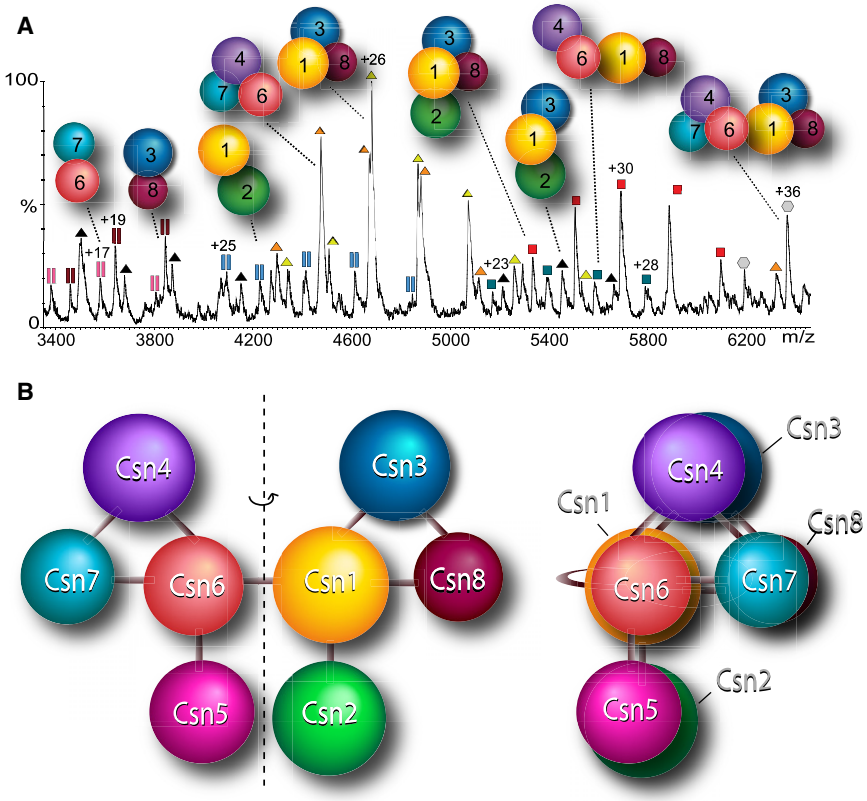


**Figure 5. Subunit Topology Map of the Human CSN Complex**

(A) An expansion of the ΔCsn5 mass spectrum recorded under harsh conditions to induce subcomplex formation labeled with the topological arrangement of subunits deduced from our interaction network.

(B) The protein-protein interaction map of the eight-subunit complex is generated after integrating the MS and tandem MS data and applying the list of identified subcomplexes to the network inference algorithm SUMMIT. Two clusters are clearly observed: Csn1/2/3/8 and Csn4/5/6/7. Only one interaction between Csn1 and Csn6 links the two modules. Within each module (Csn1/3/8 or Csn4/6/7) each subunit forms interaction with the other two, whereas Csn2 and Csn5, the most peripheral subunits, form interactions with only one subunit. A clear symmetrical modularity of the two clusters is revealed.

essential role of the subunits Csn1 and Csn6. From our topological model, this can be rationalized by their central location. Both subunits provide the stable interactions that link the two protein modules. Also of interest for biogenesis is the observation that the seven-component ΔCsn5 complex could not incorporate Csn5 under the conditions of our experiment. However, we could clearly detect an interaction between the monomeric Csn5 subunit and the trimer Csn4/6/7 (Figure 4B) and between Csn1/2/3 and Csn4/6/7 (Figure 4A). These results suggest that in the course of assembly, interactions within each module are generated initially, before interactions between the two modules.

Despite the accumulating data regarding the CSN complex, a key question arises as to how the CSN simultaneously regulates multiple pathways. Our observation that the complex is maintained, intact in solution, without the peripheral subunits (Csn2, Csn5, Csn7, and Csn8) suggests that these subunits have independent roles in many pathways. This idea is supported by the fact that individual CSN subunits have been identified in interaction with a diverse set of proteins (reviewed in Schwechheimer, 2004; Wei and Deng, 2003). Moreover, previous studies indicate that multiple CSN-independent forms can be found in complexes of molecular mass lower than the intact complex (mini-CSNs) (Karniol et al., 1999; Mundt et al., 2002; Oron et al., 2002; Serino et al., 1999; Tomoda et al., 2002; Wang et al., 2002b). In particular, Csn4 and Csn7 readily dissociate in our experiments, and have been found in subcomplexes that appear to be independent of Csn1 in *Arabidopsis* (Karniol et al., 1999; Serino et al., 1999; Wang et al., 2002a) and in *Drosophila* (Oron et al., 2002). Considering both these observations and our data, it seems likely that each of the modules Csn1/2/3/8 and Csn4/5/6/7 or their smaller triads Csn1/3/8 and Csn4/6/7 have an independent existence. Although the relevance of these mini-CSNs is yet to be defined, their structural integrity is readily observed, enabling us to propose that facile dissociation of the intact complex leads to a plethora of subcomplexes that could well provide a rationale for the multifunctionality of the CSN in vivo.

The modular composition of the COP9 signalosome can also explain the fact that some subunits of the complex are apparently missing in lower eukaryotic organisms. For example, in *Candida albicans*, *Cyanidioschyzon merolae*, and *Saccharomyces cerevisiae* (Chang and Schwechheimer, 2004; Maytal-Kivity et al., 2002a), only four PCI proteins (Csn1, Csn2, Csn3, and Csn7, or their derivatives) plus one MPN protein (Csn5) have been identified. However, these five subunits are sufficient to occupy all specific positions within the module, and it is reasonable to speculate that three of the subunits appear twice in the intact complex. Interestingly, within each module the two peripheral subunits, Csn2 and Csn5, are the most conserved, with over 60% identity between animal and plants (Wei and Deng, 2003). These subunits form extensive interactions with associated proteins (reviewed in Schwechheimer, 2004; Wei and Deng, 2003) in accord with their exposed position. Moreover, in solution in the absence of Csn5, Csn2 readily dissociates from the complex, suggesting a transient interaction between the two subunits. The observation that Csn4/6/7 dissociates readily in the absence of Csn5, but remains assembled in the presence of Csn5, further supports interactions between the two modules. Together these observations imply that transient interactions occur between the two modules, presumably mediated through flexibility in Csn1–6 interactions (Figure 5B).

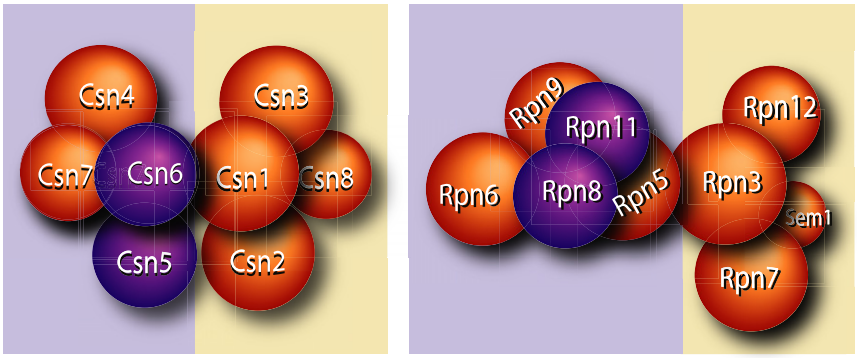


**Figure 6. Structural Organization of the CSN and the 19S Lid Complexes**
The subunit organization map of the CSN (left) and the 19S lid (right) are colored according to signature domains (PCI domains in orange and MPN domain in purple). The two modules that compose the complex are highlighted by the yellow and lilac boxes: Csn 4/5/6/7 and Rpn5/6/8/9/11 versus Csn1/2/3/8 and Rpn3/7/12/Sem1.

Given the remarkable genetic homology shared between the CSN, 19S lid, and the eIF3 complexes, we compared their structural similarity. Recent reports of the interactions maps of the 19S lid (Sharon et al., 2006) and eIF3 complexes (Zhou et al., 2008) using emerging MS approaches have shown a modular composition for all three complexes. Two protein modules comprise the 19S lid and CSN complexes (Figure 6; Figure S3 and Table S1), whereas the larger eIF3 complex is built from three structural modules. Each of the modules generated in solution contains between three and five proteins. Stable interactions between two protein subunits connect the modules, forming a relatively weak association and a possible flexible hinge region. Remarkably, the two MPN-domain-containing subunits (Rpn8/11, Csn5/6 and eIF3f/h) interact directly in all three complexes. It is noteworthy that for the CSN and 19S lid the active MPN+/JAMM subunits (Rpn11 and Csn5) are exposed whereas the other MPN subunits (Rpn8 and Csn6) occupy a central position. A further observation is that fewer subunits are found at substoichiometric levels in the 19S lid (Rpn6) than in the CSN (Csn2, Csn5, and Csn8). This is consistent with the view that dissociation of subunits from the CSN might be a feature of its ability to regulate multiple pathways. Moreover, both the eIF3 and the 19S lid complexes appear to be significantly more stable than the CSN. The multiple subcomplexes and substoichiometric binding observed here for the CSN, in contrast to the other PCI complexes, supports our hypothesis that adaptation of its subunit composition is linked to the capacity of the CSN to perform its many functional roles in vivo.

## EXPERIMENTAL PROCEDURES

### Complex Formation

The eight-subunit human COP9 complex was reconstituted by coexpression in *E. coli* (see Supplemental Experimental Procedures for subunits sequences). Three CSN subunits were coexpressed in one vector, Csn1/2/3 and Csn4/6/7, whereas Csn5 and Csn8 were expressed independently. The complex was reconstituted by incubating the purified subcomplexes and individual subunits in equimolar ratios. The reconstituted eight-subunit complex showed a robust catalytic activity in deconjugating Nedd8 from a Cul1-Rbx1 complex (Figure S1).

### Coupling Protein Identification and Accurate Mass Measurement

We have established an approach for individual subunit separation and simultaneous sequence and mass determination. In this method, two identical liquid chromatography (LC) separation runs are performed:

i) an online separation coupled to an ESI-Q-TOF (Q-star) MS for molecular weight determination of individual subunits; and

ii) an offline LC separation coupled to a probot microfraction collector, followed by on-plate tryptic digestion, for matrix-assisted laser desorption/ionization time-of-flight (MALDI-TOF) analysis and protein database search for subunit identification.

Because both runs produce the same LC chromatogram, the data can be integrated to yield a specific protein identity and mass for each isolated peak. In practice, conditions for efficient LC separation using a LC-Packings Ultimate System (Dionex, Sunnyvale, CA) fitted with a monolithic capillary column (Dionex), 200 μm i.d. × 5 cm at a flow rate of 3 μl/min, were set up by using a mixture of known proteins that mimic the proteins present in a large protein assembly. Those conditions were used to separate the CSN complex into individual subunits. Following equilibration at 90% solvent A (water/acetonitrile 98:2, 0.05% trifluoroacetic acid [TFA]) and 10% solvent B (water/acetonitrile 20:90, 0.04% TFA), separation was achieved using a linear gradient of 30% to 70% B in 20 min. The column effluent passed through a capillary UV detector (set at 280 nm for detection). In both chromatographic runs 100 pmol of the seven-subunit CSN complex (excluding Csn5) was loaded. Eluted proteins were analyzed first online by a QSTAR-XL mass spectrometer (Applied Biosystems, Foster City, CA) using the following experimental parameters: capillary voltage, up to 5 kV; declustering potential, 30 V; focusing potential, 145 V; second declustering potential, 12 V; microchannel plate 2350 V. Before the second LC run, a 4700 MALDI plate was prespotted with 0.5 μl trypsin (0.16 μg/μl, Promega, Madison, WI) and allowed to air dry. Subsequently LC fractions were deposited onto the MALDI plate at 30 s intervals (~1.5 μl/spot). Samples were overlaid with 0.5 μl 25 mM ammonium bicarbonate (pH 7.8) and incubated in a humidifier for 10 min for on-plate tryptic digestion. The digestion was terminated by the addition of 0.6 μl α-cyano-4-hydroxycinnamic acid matrix at 10 mg/ml in 50:50 water:acetonitrile with 0.1% TFA v:v. After digestion mass spectra were recorded on a 4700 Proteomics analyzer with MALDI-TOF optics (Applied Biosystems), using a 200 Hz frequency-triple Nd:YAG laser operating at a wavelength of 355 nm. Database searching was performed against the NCBInr protein database using GPS Explorer (Applied Biosystems).

For the accurate mass determination of the individual Csn5 subunits, purified singly expressed subunits were washed and eluted from a $C_4$ ZipTip column (Millipore) under denaturing conditions (50% acetonitrile and 0.1% formic acid). Mass spectrum was recorded on a QSTAR XL mass spectrometer. Because of the observed similarity in mass of Csn3 and Csn4 (118 Da) that precludes unambiguous assignment of the intact complex and subcomplexes, we used a modified strain of Csn3 that gave a mass difference of 785 Da (Table 1). In addition, we analyzed complexes in which either Csn7a or Csn7b are incorporated. Likewise, two different strains of Csn6 were used.

### MS of the CSN Complexes and Subcomplexes

For analysis of both the intact CSN complex and the seven-subunit complex (excluding Csn5) as well as smaller subcomplexes, mass spectra were acquired on a high mass quadrupole TOF-type instrument adapted for a QSTAR XL platform (Chernushevich and Thomson, 2004; Sobott et al., 2002). Before mass spectrometry, 25 μl of the 10–70 μM solution was buffer-exchanged up to three times into 1 M ammonium acetate (pH 7.5) using Micro Biospin 6 columns (Bio-Rad), and 2 μl aliquots were introduced via

nanoflow capillaries prepared in-house. The conditions within the mass spectrometer were adjusted to preserve noncovalent interactions. The mass spectrometer was operated at a capillary voltage of 1200 V and a declustering potential of 150 V (focusing potential, 250 V; second declustering potential, 15V; collision energy, up to 200 V; microchannel plate, 2350 V). The intact complexes were disrupted through the addition of 5%–12.5% methanol (v/v) or via in-source collision-induced dissociation. The assembly of individually expressed subunits Csn5 and Csn8 with the coexpressed subcomplexes Csn1/2/3 and Csn4/6/7 was investigated after mixing equimolar quantities followed by 10–60 min incubation at 37°C. In MS/MS the relevant m/z value was selected in the quadrupole and argon was used as a collision gas at maximum pressure with collision energy ranging from 100 to 200 V. All spectra were calibrated externally by using a solution of cesium iodide (100 mg/ml). Spectra are shown here with minimal smoothing and without background subtraction.

### Assignment of the Subcomplexes and Building the Interaction Network

Two hundred mass spectra and tandem mass spectra were analyzed to give molecular masses for the various charge states of the subcomplexes and complexes. Compositions of the subcomplexes were assigned using an iterative search algorithm that explores all possible combinations of the experimentally determined subunit masses within a given error limit (Taverner et al., 2008). Where ambiguity in the assignment of a subcomplex existed, MS/MS data was used to discriminate the different possibilities. A list of 35 subcomplexes ranging from dimers to heptamers was generated. These subcomplexes were assigned unambiguously and no conflicts were found between the many datasets recorded under the various MS and solution phase conditions. We then explored all possible networks consistent with the subcomplexes identified using the network inference algorithm SUMMIT (Taverner et al., 2008). This algorithm examines all potential interactions and optimizes the network with respect to the shortest interaction path.

## SUPPLEMENTAL DATA

Supplemental Data include three figures, one table, and Supplemental Experimental Procedures, and can be found with this article online at http://www.cell.com/structure/supplemental/S0969-2126(08)00417-6.

## ACKNOWLEDGMENTS

We thank Sarah Maslen for valuable assistance. M.S. and C.V.R. are grateful for funding from Royal Society, the BBSRC, and the Walters Kundert Trust.

Received: August 1, 2008
Revised: September 10, 2008
Accepted: October 13, 2008
Published: January 13, 2009

## REFERENCES

Ambroggio, X.I., Rees, D.C., and Deshaies, R.J. (2004). JAMM: a metalloprotease-like zinc site in the proteasome and signalosome. PLoS Biol. *2*, E2.

Aravind, L., and Ponting, C.P. (1998). Homologues of 26S proteasome subunits are regulators of transcription and translation. Protein Sci. *7*, 1250–1254.

Bemis, L., Chan, D.A., Finkielstein, C.V., Qi, L., Sutphin, P.D., Chen, X., Stenmark, K., Giaccia, A.J., and Zundel, W. (2004). Distinct aerobic and hypoxic mechanisms of HIF-alpha regulation by CSN5. Genes Dev. *18*, 739–744.

Benesch, J.L., Aquilina, J.A., Ruotolo, B.T., Sobott, F., and Robinson, C.V. (2006). Tandem mass spectrometry reveals the quaternary organization of macromolecular assemblies. Chem. Biol. *13*, 597–605.

Benesch, J.L., Ruotolo, B.T., Simmons, D.A., and Robinson, C.V. (2007). Protein complexes in the gas phase: technology for structural genomics and proteomics. Chem. Rev. *107*, 3544–3567.

Chamovitz, D.A., and Segal, D. (2001). JAB1/CSN5 and the COP9 signalosome. A complex situation. EMBO Rep. *2*, 96–101.

Chamovitz, D.A., Wei, N., Osterlund, M.T., von Arnim, A.G., Staub, J.M., Matsui, M., and Deng, X.W. (1996). The COP9 complex, a novel multisubunit nuclear regulator involved in light control of a plant developmental switch. Cell *86*, 115–121.

Chang, E.C., and Schwechheimer, C. (2004). ZOMES III: the interface between signalling and proteolysis. Meeting on The COP9 Signalosome, Proteasome and eIF3. EMBO Rep. *5*, 1041–1045.

Chernushevich, I.V., and Thomson, B.A. (2004). Collisional cooling of large ions in electrospray mass spectrometry. Anal. Chem. *76*, 1754–1760.

Cope, G.A., and Deshaies, R.J. (2003). COP9 signalosome: a multifunctional regulator of SCF and other cullin-based ubiquitin ligases. Cell *114*, 663–671.

Cope, G.A., Suh, G.S., Aravind, L., Schwarz, S.E., Zipursky, S.L., Koonin, E.V., and Deshaies, R.J. (2002). Role of predicted metalloprotease motif of Jab1/Csn5 in cleavage of Nedd8 from Cul1. Science *298*, 608–611.

Damoc, E., Fraser, C.S., Zhou, M., Videler, H., Mayeur, G.L., Hershey, J.W., Doudna, J.A., Robinson, C.V., and Leary, J.A. (2007). Structural characterization of the human eukaryotic initiation factor 3 protein complex by mass spectrometry. Mol. Cell. Proteomics *6*, 1135–1146.

Deng, X.W., Dubiel, W., Wei, N., Hofmann, K., Mundt, K., Colicelli, J., Kato, J., Naumann, M., Segal, D., Seeger, M., et al. (2000). Unified nomenclature for the COP9 signalosome and its subunits: an essential regulator of development. Trends Genet. *16*, 202–203.

Deshaies, R.J., and Meyerowitz, E. (2000). COP1 patrols the night beat. Nat. Cell Biol. *2*, E102–E104.

Dohmann, E.M., Kuhnle, C., and Schwechheimer, C. (2005). Loss of the CONSTITUTIVE PHOTOMORPHOGENIC9 signalosome subunit 5 is sufficient to cause the cop/det/fus mutant phenotype in Arabidopsis. Plant Cell *17*, 1967–1978.

Glickman, M.H., Rubin, D.M., Coux, O., Wefes, I., Pfeifer, G., Cjeka, Z., Baumeister, W., Fried, V.A., and Finley, D. (1998). A subcomplex of the proteasome regulatory particle required for ubiquitin-conjugate degradation and related to the COP9-signalosome and eIF3. Cell *94*, 615–623.

Gusmaroli, G., Figueroa, P., Serino, G., and Deng, X.W. (2007). Role of the MPN subunits in COP9 signalosome assembly and activity, and their regulatory interaction with Arabidopsis Cullin3-based E3 ligases. Plant Cell *19*, 564–581.

Harari-Steinberg, O., and Chamovitz, D.A. (2004). The COP9 signalosome: mediating between kinase signaling and protein degradation. Curr. Protein Pept. Sci. *5*, 185–189.

Hernandez, H., Dziembowski, A., Taverner, T., Seraphin, B., and Robinson, C.V. (2006). Subunit architecture of multimeric complexes isolated directly from cells. EMBO Rep. *7*, 605–610.

Hinnebusch, A.G. (2006). eIF3: a versatile scaffold for translation initiation complexes. Trends Biochem. Sci. *31*, 553–562.

Hofmann, K., and Bucher, P. (1998). The PCI domain: a common theme in three multiprotein complexes. Trends Biochem. Sci. *23*, 204–205.

Huang, X., Hetfeld, B.K., Seifert, U., Kahne, T., Kloetzel, P.M., Naumann, M., Bech-Otschir, D., and Dubiel, W. (2005). Consequences of COP9 signalosome and 26S proteasome interaction. FEBS J. *272*, 3909–3917.

Kapelari, B., Bech-Otschir, D., Hegerl, R., Schade, R., Dumdey, R., and Dubiel, W. (2000). Electron microscopy and subunit-subunit interaction studies reveal a first architecture of COP9 signalosome. J. Mol. Biol. *300*, 1169–1178.

Karniol, B., Malec, P., and Chamovitz, D.A. (1999). Arabidopsis FUSCA5 encodes a novel phosphoprotein that is a component of the COP9 complex. Plant Cell *11*, 839–848.

Li, L., and Deng, X.W. (2003). The COP9 signalosome: an alternative lid for the 26S proteasome? Trends Cell Biol. *13*, 507–509.

Mann, M., Hendrickson, R.C., and Pandey, A. (2001). Analysis of proteins and proteomes by mass spectrometry. Annu. Rev. Biochem. *70*, 437–473.

Maytal-Kivity, V., Piran, R., Pick, E., Hofmann, K., and Glickman, M.H. (2002a). COP9 signalosome components play a role in the mating pheromone response of S. cerevisiae. EMBO Rep. *3*, 1215–1221.

  

Maytal-Kivity, V., Reis, N., Hofmann, K., and Glickman, M.H. (2002b). MPN+, a putative catalytic motif found in a subset of MPN domain proteins from eukaryotes and prokaryotes, is critical for Rpn11 function. BMC Biochem. *3*, 28.

McKay, A.R., Ruotolo, B.T., Ilag, L.L., and Robinson, C.V. (2006). Mass measurements of increased accuracy resolve heterogeneous populations of intact ribosomes. J. Am. Chem. Soc. *128*, 11433–11442.

Mundt, K.E., Liu, C., and Carr, A.M. (2002). Deletion mutants in COP9/signalosome subunits in fission yeast *Schizosaccharomyces pombe* display distinct phenotypes. Mol. Biol. Cell *13*, 493–502.

Nordgard, O., Dahle, O., Andersen, T.O., and Gabrielsen, O.S. (2001). JAB1/CSN5 interacts with the GAL4 DNA binding domain: a note of caution about two-hybrid interactions. Biochimie *83*, 969–971.

Oron, E., Mannervik, M., Rencus, S., Harari-Steinberg, O., Neuman-Silberberg, S., Segal, D., and Chamovitz, D.A. (2002). COP9 signalosome subunits 4 and 5 regulate multiple pleiotropic pathways in Drosophila melanogaster. Development *129*, 4399–4409.

Peng, Z., Shen, Y., Feng, S., Wang, X., Chitteti, B.N., Vierstra, R.D., and Deng, X.W. (2003). Evidence for a physical association of the COP9 signalosome, the proteasome, and specific SCF E3 ligases in vivo. Curr. Biol. *13*, R504–R505.

Peth, A., Berndt, C., Henke, W., and Dubiel, W. (2007). Downregulation of COP9 signalosome subunits differentially affects the CSN complex and target protein stability. BMC Biochem. *8*, 27.

Richardson, K.S., and Zundel, W. (2005). The emerging role of the COP9 signalosome in cancer. Mol. Cancer Res. *3*, 645–653.

Schwechheimer, C. (2004). The COP9 signalosome (CSN): an evolutionary conserved proteolysis regulator in eukaryotic development. Biochim. Biophys. Acta *1695*, 45–54.

Schwechheimer, C., and Deng, X.W. (2001). COP9 signalosome revisited: a novel mediator of protein degradation. Trends Cell Biol. *11*, 420–426.

Serino, G., Tsuge, T., Kwok, S., Matsui, M., Wei, N., and Deng, X.W. (1999). Arabidopsis cop8 and fus4 mutations define the same gene that encodes subunit 4 of the COP9 signalosome. Plant Cell *11*, 1967–1980.

Sharon, M., and Robinson, C.V. (2007). The role of mass spectrometry in structure elucidation of dynamic protein complexes. Annu. Rev. Biochem. *76*, 167–193.

Sharon, M., Taverner, T., Ambroggio, X.I., Deshaies, R.J., and Robinson, C.V. (2006). Structural organization of the 19S proteasome lid: insights from MS of intact complexes. PLoS Biol. *4*, e267.

Sobott, F., Hernandez, H., McCammon, M.G., Tito, M.A., and Robinson, C.V. (2002). A tandem mass spectrometer for improved transmission and analysis of large macromolecular assemblies. Anal. Chem. *74*, 1402–1407.

Spain, B.H., Bowdish, K.S., Pacal, A.R., Staub, S.F., Koo, D., Chang, C.Y., Xie, W., and Colicelli, J. (1996). Two human cDNAs, including a homolog of Arabidopsis FUS6 (COP11), suppress G-protein- and mitogen-activated protein kinase-mediated signal transduction in yeast and mammalian cells. Mol. Cell. Biol. *16*, 6698–6706.

Taverner, T., Hernández, H., Sharon, M., Ruotolo, B.T., Matak-Vinkovic, D., Devos, D., Russell, R.B., and Robinson, C.V. (2008). Subunit architecture of intact protein complexes from mass spectrometry and homology modeling. Acc. Chem. Res. *41*, 617–627.

Tomoda, K., Kubota, Y., Arata, Y., Mori, S., Maeda, M., Tanaka, T., Yoshida, M., Yoneda-Kato, N., and Kato, J.Y. (2002). The cytoplasmic shuttling and subsequent degradation of p27Kip1 mediated by Jab1/CSN5 and the COP9 signalosome complex. J. Biol. Chem. *277*, 2302–2310.

Tsuge, T., Matsui, M., and Wei, N. (2001). The subunit 1 of the COP9 signalosome suppresses gene expression through its N-terminal domain and incorporates into the complex through the PCI domain. J. Mol. Biol. *305*, 1–9.

Uetz, P., Giot, L., Cagney, G., Mansfield, T.A., Judson, R.S., Knight, J.R., Lockshon, D., Narayan, V., Srinivasan, M., Pochart, P., et al. (2000). A comprehensive analysis of protein-protein interactions in Saccharomyces cerevisiae. Nature *403*, 623–627.

van den Heuvel, R.H., and Heck, A.J. (2004). Native protein mass spectrometry: from intact oligomers to functional machineries. Curr. Opin. Chem. Biol. *8*, 519–526.

Voges, D., Zwickl, P., and Baumeister, W. (1999). The 26S proteasome: a molecular machine designed for controlled proteolysis. Annu. Rev. Biochem. *68*, 1015–1068.

von Arnim, A.G. (2003). On again-off again: COP9 signalosome turns the key on protein degradation. Curr. Opin. Plant Biol. *6*, 520–529.

Wang, X., Kang, D., Feng, S., Serino, G., Schwechheimer, C., and Wei, N. (2002a). CSN1 N-terminal-dependent activity is required for Arabidopsis development but not for Rub1/Nedd8 deconjugation of cullins: a structure-function study of CSN1 subunit of COP9 signalosome. Mol. Biol. Cell *13*, 646–655.

Wang, Y., Devereux, W., Stewart, T.M., and Casero, R.A., Jr. (2002b). Polyamine-modulated factor 1 binds to the human homologue of the 7a subunit of the Arabidopsis COP9 signalosome: implications in gene expression. Biochem. J. *366*, 79–86.

Wei, N., Chamovitz, D.A., and Deng, X.W. (1994). Arabidopsis COP9 is a component of a novel signaling complex mediating light control of development. Cell *78*, 117–124.

Wei, N., and Deng, X.W. (2003). The COP9 signalosome. Annu. Rev. Cell Dev. Biol. *19*, 261–286.

Wei, N., Tsuge, T., Serino, G., Dohmae, N., Takio, K., Matsui, M., and Deng, X.W. (1998). The COP9 complex is conserved between plants and mammals and is related to the 26S proteasome regulatory complex. Curr. Biol. *8*, 919–922.

Wolf, D.A., Zhou, C., and Wee, S. (2003). The COP9 signalosome: an assembly and maintenance platform for cullin ubiquitin ligases? Nat. Cell Biol. *5*, 1029–1033.

Yahalom, A., Kim, T.H., Roy, B., Singer, R., von Arnim, A.G., and Chamovitz, D.A. (2008). Arabidopsis eIF3e is regulated by the COP9 signalosome and has an impact on development and protein translation. Plant J. *53*, 300–311.

Zhou, M., Sandercock, A.M., Fraser, C.S., Matthew, S., Leary, J.A., Hershey, J.W., Doudna, J., and Robinson, C.V. (2008). Mass spectrometry reveals modularity and a complete subunit interaction map of the eukaryotic translation factor eIF3. Proc. Natl. Acad. Sci. USA *105*, 18139–18144.

 